Hydrogen reduction of ilmenite: Towards an in situ resource utilization demonstration on the surface of the Moon

Journal Item

Journal Pre-proof

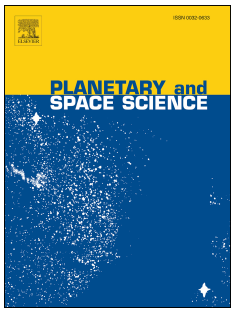

Hydrogen reduction of ilmenite: Towards an in situ resource utilization demonstration on the surface of the Moon

H.M. Sargeant, F.A.J. Abernethy, S.J. Barber, I.P. Wright, M. Anand, S. Sheridan, A. Morse

PII: S0032-0633(19)30181-3

DOI: https://doi.org/10.1016/j.pss.2019.104751

Reference: PSS 104751

To appear in: *Planetary and Space Science*

Received Date: 30 April 2019

Revised Date: 11 September 2019

Accepted Date: 18 September 2019

Please cite this article as: Sargeant, H.M., Abernethy, F.A.J., Barber, S.J., Wright, I.P., Anand, M., Sheridan, S., Morse, A., Hydrogen reduction of ilmenite: Towards an in situ resource utilization demonstration on the surface of the Moon, *Planetary and Space Science* (2019), doi: https://doi.org/10.1016/j.pss.2019.104751.

Hydrogen Reduction of Ilmenite: Towards an In Situ Resource Utilization Demonstration on the Surface of the Moon

H. M. Sargeant[1], F. A. J. Abernethy[1], S. J. Barber[1], I. P. Wright[1], M. Anand[1], S. Sheridan[1], A. Morse[1].

[1] The Open University, United Kingdom

Corresponding author: Hannah Sargeant (hannah.sargeant@open.ac.uk)

Abstract

Water is one of the most vital resources required for future space exploration. By obtaining water from lunar regolith, humans are one step closer to being independent of Earth's resources enabling longer term exploration missions. Hydrogen reduction of ilmenite is often proposed as a technique for producing water on the Moon. ProSPA, a miniature analytical laboratory, will perform reduction of lunar soils as an In-Situ Resource Utilization (ISRU) demonstration on the lunar surface. The technique used by ProSPA will be useful for prospecting payloads with limited mass and power resources. This work considers the development and optimization of an ilmenite ($FeTiO_3$) reduction procedure for use with the ProSPA instrument. It is shown that the reaction can be performed in a static (non-flowing) system, by utilizing a cold finger to collect the water produced from the reaction. Among the investigated parameters an initial H_2:$FeTiO_3$ ratio of 1, in this case equating to a hydrogen pressure of 418 mbar, proved to be best for providing maximum yields over 4 hours when operating at 1000°C. Results indicate that a maximum yield of 3.40±0.17 wt. % O_2 can be obtained at 1000°C (with a maximum possible

yield of 10.5 wt. % O_2). When operating at higher temperatures of 1100°C the ilmenite grains undergo a subsolidus reaction resulting in the formation of ferropseudobrookite and higher yields of 4.42±0.18 wt. % O_2 can be obtained.

Keywords

#ISRU #Ilmenite #Hydrogen Reduction #Static #ProSPA #Moon

Highlights

- Demonstration of reduction of ilmenite by H_2 in a non-flowing system
- Proof of principle for an ISRU demonstration on the Moon
- Yields of up to 4.4 wt.% O_2 which is reasonable considering the constraints

1 Introduction

The availability of water poses a significant challenge for long-term crewed missions to the Moon and beyond. Each crew member requires ~4.19 kg/day of water, whilst its constituent oxygen is also vital for crew support at 0.93 kg/day (Jones & Kliss, 2010). Oxygen and hydrogen can also be used for rocket propellant to launch supplies to crews on their way to Mars (Lewis, 1993). The cost of supplying all of the water and constituent oxygen and hydrogen required for such long term exploration missions can become prohibitive. By obtaining the resources required from local materials, known as In-Situ Resource Utilization (ISRU), the costs could be lowered. The Moon was once thought to be bone-dry (e.g. Latham et al., 1970; Maxwell et al., 1970; Papike et al., 1991). However, more recent evidence suggests the presence of water in lunar samples (McCubbin et al., 2015; Barnes et al., 2014; Saal et al., 2008) and water-ice at the lunar poles (Colaprete et al., 2010; Li et al., 2018). These polar regions provide numerous

technological challenges in accessing potential frozen water deposits in terms of extreme low temperatures, lack of solar energy, and relatively unknown regolith properties (Burke, 2012). Therefore, other sources of water are being considered to meet the needs of future missions (Taylor & Carrier, 1993), such as hydrogen reduction of ilmenite, carbothermal reactions, high temperature pyrolysis, and melt regolith extraction. Of these, ilmenite reduction requires the lowest temperature and has the highest TRL (Technology Readiness Level) but it has the lowest potential yield which is strongly influenced by feedstock composition (Sanders & Larson, 2011).

Hydrogen reduction of ilmenite is a commonly considered water production technique for operation on the lunar surface because of its relatively low temperature (e.g. Christiansen et al., 1988; Gibson & Knudsen, 1985; Ness Jr et al., 1992). Ilmenite is a common lunar mineral (Papike et al., 1991) that can be reduced in the solid phase to produce water as in Eqn. 1. The state of each reactant and product is denoted as (s) solid or (g) gas:

$$\boldsymbol{FeTiO_{3(s)} + H_{2(g)} \rightleftharpoons Fe_{(s)} + TiO_{2(s)} + H_2O_{(g)}} \qquad \textbf{Eqn. 1}$$

The ilmenite reduction reaction is an equilibrium reaction and therefore requires the removal of the product water from the reaction site in order to continue to produce water. Altenberg et al. (1993) modelled how the equilibrium constant for this reaction varies with hydrogen pressure and temperature. The results showed that the equilibrium constant increases with lower pressures of hydrogen and higher temperatures, resulting in higher yields. Generally, a flow of hydrogen gas is used to reduce the ilmenite which carries away the produced water to a condenser. Dynamic systems that utilize a flow of hydrogen have been theorized for large scale water production on the Moon (Christiansen et al., 1988). More recently, ilmenite reduction

demonstrators have been built that utilize a fluidized bed or a rotating drum to ensure maximum contact between the regolith and reductant gas during the reaction (Sanders & Larson, 2011).

The yield of oxygen from ilmenite reduction is dependent on the feedstock composition. Ilmenite can readily be reduced, thanks to its high Fe^{2+} content, but other Fe^{2+} bearing minerals can also reduce, albeit generating lower yields (Allen et al., 1994). Prospecting will therefore be required to evaluate a wide range of potential regions such as high titanium mare and iron rich pyroclastic flows, requiring sample return missions or as a first step sample analysis in-situ. With the intention of national space agencies using commercial lunar landers it is likely that payloads will initially have severely constrained mass and power budgets. Prospecting with small instruments (~10 kg) will be required before committing to a large-scale demonstration plant at a single favorable location. ProSPA is an analytical instrument which has the goal of performing the first ISRU demonstration on the Moon (Barber et al., 2018). The instrument, which is being developed at The Open University, is part of the PROSPECT package that will be on board the Luna-27 mission to a high latitude region of the Moon in 2025. ProSPA will perform in situ analyses on samples of lunar regolith, potentially detect and characterize lunar volatiles, and also attempt to reduce lunar minerals, including ilmenite, to produce water. As ProSPA is an analytical instrument with mass budget limited to 10 kg, it does not have the resources for a complete ilmenite reduction system, including fluidized/rotating, recirculating hydrogen plumbing, and condenser. Instead a different approach has been taken adapting to the available hardware and the natural environment to evaluate the regolith at the landing site as a feedstock for oxygen production by reduction with hydrogen. A static process is considered where the ilmenite is exposed to hydrogen (in a closed system), while a cold finger condenses any produced water as trialled by Williams (1985), thus removing it from the reaction site and

enabling the reaction to continue to the right as written, preventing the reverse reaction taking place.

Previous work by the authors (Sargeant et al., 2019a) has shown that a static approach is viable and water can be produced from the reduction of ilmenite when a cold finger is implemented. The breadboard system used in Sargeant et al. (2019a) was not able to quantify the yields of water produced accurately, as it lacked the necessary thermal control to prevent unwanted condensation of water in cooler sections of the system.

A new breadboard model (ISRU-BDM) has been developed which provides increased thermal control to allow quantification of yields of water using the static system approach. This work discusses the design and build of the ISRU-BDM, and the experimental determination of the optimum temperature and hydrogen concentration conditions, and the associated yields.

2 Materials and Methods

The ISRU-BDM is designed to represent certain aspects of the ProSPA design; the sample oven, hydrogen supply, cold finger, mass spectrometer, and interconnecting pipework with pressure sensors.

2.1 System Design

The ISRU breadboard utilizes a heated box, where all major components that can withstand high temperatures, are placed. As the mass spectrometer cannot be placed inside the oven, it is connected instead via a heated capillary. A schematic of the ISRU-BDM is shown in Figure 1.

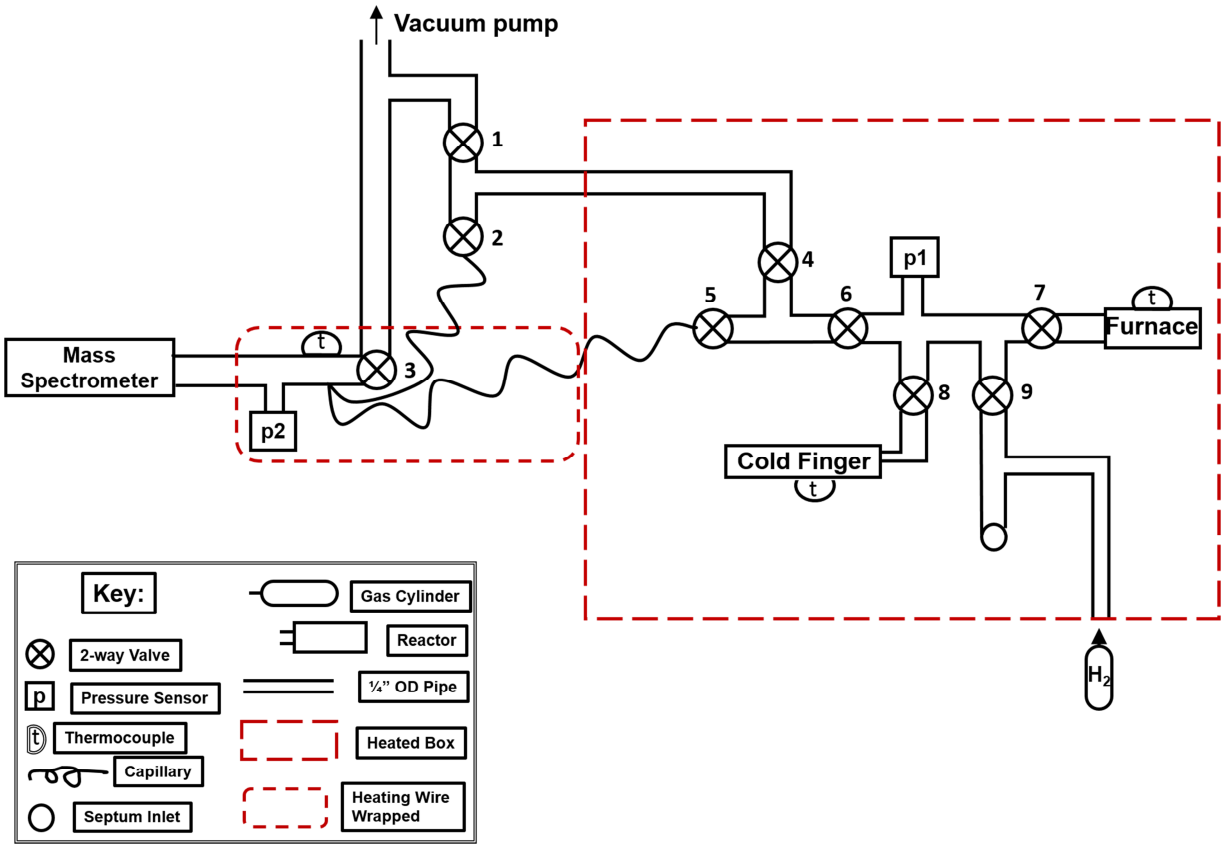

Figure 1. *ISRU breadboard schematic.*

The heated box is made from vermiculite sheets on a 100x65x75 cm aluminum frame, and is heated to ~120°C by two 2 kW oven heating elements. Swagelok® VCR fittings of 1/4 inch ID are used throughout. High temperature (up to 315°C) Swagelok® actuator valves with stainless steel spherical tips are used inside the oven to control the movement of gases. A high

temperature Kulite® diaphragm pressure sensor is used to monitor the gas pressure in the system. A compact furnace which utilizes a ceramic chamber with embedded resistance wires is used to heat samples up to 1100°C. It should be noted that a K-type thermocouple located within the furnace experienced multiple failures when operating at temperatures >1000°C. As a result, the furnace can shut down early resulting in lower yields. This was not identified in previous work by the authors causing incorrect interpretations of the data in Sargeant et al. (2019b). The thermocouple is closely monitored in the following studies to ensure all reactions are completed. The 200 mm length, 4 mm ID ceramic sample tube is placed inside the furnace before each experiment. The system is connected to an outer manifold, where the mass spectrometer is located, via an exhaust pipe and a capillary tube. All outer components of the manifold, except for the mass spectrometer, are heated to 100°C with resistance heating wire. The outer manifold hosts the Hiden HPR-20 quadrupole mass spectrometer via a crimped stainless steel capillary inlet. A novel cold finger design was developed to provide increased thermal control, as compared to the design used in Sargeant et al. (2019a), when trapping and releasing gases (See supplementary material Figure S1). The finished system is shown in Figure 2.

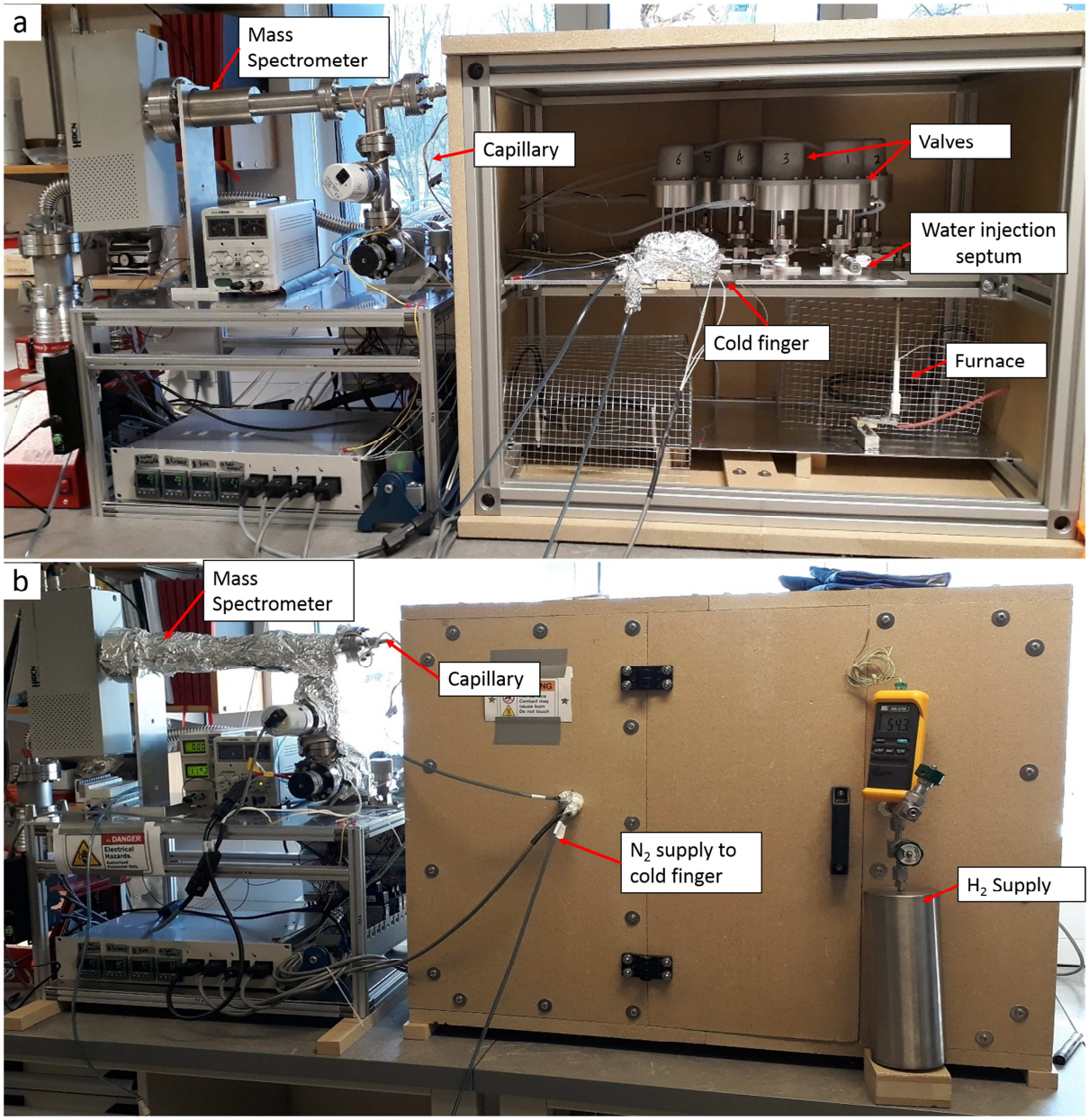

Figure 2. *a.) Front image of the ISRU breadboard with the oven door removed. b.) Front image of the ISRU breadboard with the oven door attached. The entire system is ~2 m wide and 1 m tall.*

2.2 Experimental Procedure

The evening before each experiment, the oven in which the system is placed is set to heat to 120°C. This guarantees the manifold is at 120°C before an experiment can begin, minimizing the condensation of any water onto the pipework. The ilmenite used in this work is ~95% pure with an average particle diameter of ~170 μm (Sargeant et al., 2019a). The ~45 mg ilmenite sample is placed into a ceramic tube and sealed onto the system at valve 7 using an O-ring tube fitting (Figure 1). The ilmenite mass was selected as it is the approximate sample size for ProSPA ovens. Each experiment is controlled using LabView software which allows a high level of automation and therefore consistency between each run.

A summary of the operational conditions of the ISRU-BDM during the experiment is shown in Table 1, whilst a graphical representation of the procedure is outlined in the supplementary material Figure S2. The following procedure is performed for each experiment. A 1 hour bake-out procedure is performed at the start of each program where the furnace is heated to 500°C and open to the vacuum pump in order to remove any volatiles from the sample as in Sargeant et al. (2019a). Meanwhile the cold finger is isolated from the pumping system and set to -80°C chosen because >99.99% of any water produced in the following reactions should condense at this temperature (calculated assuming a saturation vapor limit of < 0.0044 mbar, which is 0.01% of the potential water produced during the following experiments). Next, the furnace is isolated and set to a pre-defined reaction temperature. At this point, the program pauses until the hydrogen supply is manually opened and hydrogen fills the defined volume until the required pressure is reached. The system is then closed and the furnace and cold finger are opened to the rest of the system. The ilmenite in the furnace is then able to react with the hydrogen, where any produced water diffuses through the system before condensing at the cold finger. The pressure in the system is monitored every minute during the reaction as the samples are left to react for 4 hours.

A reaction time of 4 hours was selected as a reasonable time frame for such experiments to be performed on the Luna-27 mission. After the reaction, the system is evacuated of any remaining gases and the furnace is left to cool for 2 hours to reach 120°C. Finally, the cold finger is heated to 120°C and the condensed water sublimates into the system where the pressure is monitored.

Experimental stage	System conditions				
	Operational volume (m^3)	Cold finger temperature (°C)	Furnace temperature (°C)	Heated box temperature (°C)	External manifold temperature (°C)
Bake-out	4.73E-05±1.93E-07	-80	500	120	100
H_2 addition	1.19E-05±9.93E-08	-80	500	120	100
Reduction reaction	2.19E-05±1.49E-07	-80	Reaction temperature	120	100
Water release	2.19E-05±1.49E-07	120	120	120	100

Table 1. *Operational conditions of the ISRU-BDM during each experimental stage.*

To confirm that water has been produced during the reaction, the mass spectrometer is used to sample the released volatiles from the cold finger. The mass spectrometer requires at least 1 hour for the baseline readings to normalize without changing the operational volume. Therefore the mass spectrometer cannot be used to monitor the reaction because there are operational volume changes that occur just before the reaction phase that will affect the baseline spectra. The capillary between valve 2 and the mass spectrometer proved to be most effective at sampling the vapor for analysis at the mass spectrometer. After an ilmenite reduction reaction is performed

and the volatiles are released from the cold finger, the volatiles are re-condensed at the cold finger. The mass spectrometer is used to scan across m/z values of 1-50 and the operational volume is expanded to include the capillary at valve 2. The cold finger is then heated to 120°C to sublimate the volatiles which are then sampled by the mass spectrometer.

2.3 Calculating Yields

The pressure changes measured for each experiment are corrected for system temperature by multiplying by the relevant k_T factor (see supplementary material S1), and then corrected further by subtracting the corrected blank pressure change. The pressure changes are converted into the quantity of hydrogen that has reacted, n_h, and the quantity of water produced, n_w, by applying the ideal gas law as follows:

$$\boldsymbol{n_{h|w} = \frac{pV}{RT}} \qquad \textbf{(Eqn. 2)}$$

where the corrected pressure, p, is multiplied by the volume of the system, V, which is defined in Table 1, then dividing by the ideal gas constant, R, and the temperature of the system, T (K), also defined in Table 1.

The rate of water production, R_w, is considered as a way to compare each experiment and determine the optimum reaction procedure, and can be calculated as follows:

$$\boldsymbol{R_w = \frac{V_w}{t} = \frac{m_w}{\rho_w t} = \frac{n_w M_w}{\rho_w t}} \qquad \textbf{(Eqn. 3)}$$

where V_w is the volume of water produced, t is the time over which the rate of production is being measured, m_w is the mass of water produced, ρ_t is the density of water under S.T.P (Standard Temperature and Pressure, 273.15 K and 101.325 kPa respectively) conditions, n_w is the quantity of water produced as calculated from the water release phase, and M_w is the molar mass of water.

The yield of the reduction reaction is described by the wt. % of oxygen extracted compared to the total sample mass and is therefore the ratio between the mass of oxygen produced, m_o, and the mass of ilmenite, m_{ilm}, in the sample. Yield can therefore be calculated as follows:

$$\boldsymbol{wt.\%\, O_2 = \frac{m_o}{m_{ilm}} = \frac{m_w M_o}{m_{ilm} M_w} = \frac{n_w M_o}{m_{ilm}}} \quad \textbf{(Eqn. 4)}$$

where M_o is the molar mass of oxygen.

The maximum theoretical yield of oxygen (in the form of water) from the ilmenite reduction process is 10.5 wt. % O_2, whilst up to 31.6 wt.% O_2 can be produced from ilmenite reduction and the complete reduction of the rutile product. It should be noted that yields are generally calculated using the n_w value calculated from the pressure rise measured during the water release phase (Eqn. 2). The pressure change during the reduction reaction has the potential to be affected by the production of other reaction products, whereas the pressure rise during the water release phase should solely represent the release of water from the cold finger. However, in order to understand how the yield varies during the reaction phase, the quantity of water produced is equated to the amount of hydrogen removed from the system, as hydrogen converts to water in a 1:1 reaction. Therefore the n_h value, calculated from the change in hydrogen pressure, is used as a proxy for n_w when analyzing the rate of water production during the reaction phase.

Another way to understand the efficiency of the reactions performed is to calculate the extent of the reduction reaction, ξ (%). The reduction extent is derived from the ratio of the mass of oxygen removed in the reaction, m_o, w.r.t. the mass of oxygen that could be extracted, $m_{o,max}$ and is calculated as follows:

$$\xi = \frac{m_o}{m_{o,max}} = \frac{m_o M_{ilm}}{M_o m_{ilm}} \quad \textbf{(Eqn. 5)}$$

3 Results

3.1 Temperature Studies

The ilmenite reduction reaction temperature was varied from 850 to 1100°C. The amount of hydrogen used in each reaction was selected to be 0.3 mmol which is equivalent to the amount of ilmenite in each sample. The amount of hydrogen at the start of the reaction should therefore be 420 mbar, however, the operational procedure is susceptible to an 'overshoot' in the addition of hydrogen and therefore the hydrogen pressure can be higher than 420 mbar by as much as 50 mbar (an extra 0.036 mmol of hydrogen). The pressure was recorded during the reduction reaction and water release phases of each experiment. The pressure drop recorded during the reaction phase is recorded and correlates to the amount of water trapped at the cold finger. The pressure rise is then recorded during the water release phase, and correlates with the amount of water retrieved by the trap and release process. A blank reading was run for comparison where an empty sample tube was reacted at 1000°C.

3.1.2 Reaction Pressures

During the 4 hour reaction phase, the change in pressure is greater for higher temperatures, indicating the reaction proceeds at a faster rate (Figure 3a). A small drop in pressure (temperature corrected to 6.1 mbar) is recorded in the blank reading which is from the flow through the capillary to the mass spectrometer. The resulting pressure rise from the sublimation of water from the cold finger is shown in Figure 3b. The pressure data and calculated amount of hydrogen used in the reaction, n_h, is shown in supplementary material Table S2. The n_h value is

calculated using Eqn. 2 where the pressure readings have been corrected by the k_T factor and have subtracted the equivalent blank reading of 6.1 mbar.

The pressure rise from the water release phase is shown in Figure 3b. The results show that more water is released form the cold finger for reactions that occurred at higher temperatures. The pressure changes recorded in the water release phase are as much as 10% less than that measured during the reaction phase. The pressure data for the water release phase is shown in supplementary material Table S3.

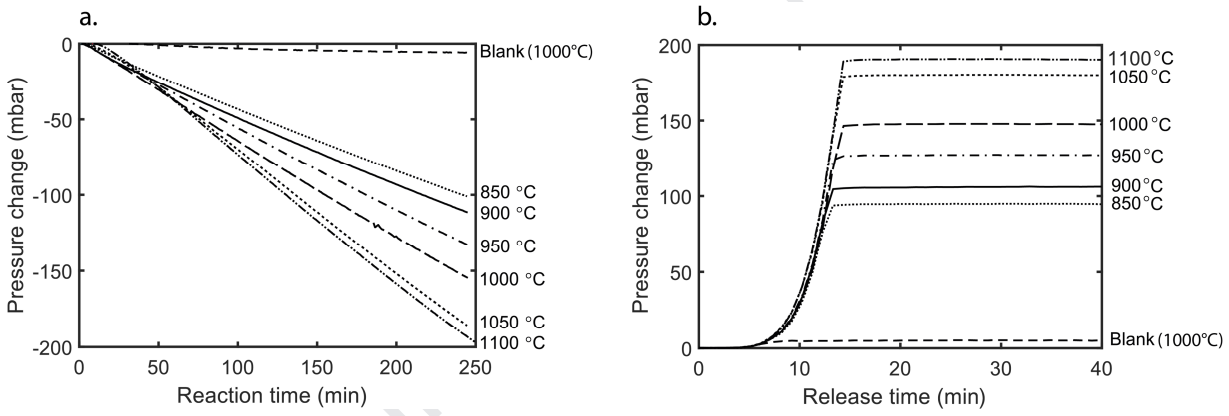

Figure 3. *Pressure change during a.) the ilmenite reduction reaction, and b.) the volatile release phase, for reaction temperatures of 850°C to 1100°C. Results shown are not corrected for the blank reading.*

The breakdown of water production rates during the reaction phase, and the total amount of water produced as calculated from the water release phase are shown in Table 2. The amount of hydrogen removed from the system during each hour, n_h, is used in Eqn. 3 as a substitute for n_w to calculate the water production rate for each hour. The total water production rate for the entire reaction (0-4 hrs) is calculated from n_w obtained from the water release phase pressure data. It can be seen that water production rate increases with temperature where the maximum rate is

achieved at 1100°C with a peak of 0.65±0.08 μl hr^{-1}. The reaction rate does not appear to significantly change across the 4 hour reaction time at each temperature suggesting the reaction is not near completion. Uncertainties are calculated using the propagation of uncertainties from the manifold temperature (±5°C), volume (Table 1), and pressure values (±6.2 mbar). The temperature uncertainty is derived from the variation in manifold temperature in the heated box, the volume uncertainty is derived from the standard deviation in volume calculations performed from the expansion of gases in the system, and the pressure uncertainty is derived from the standard deviation of pressures calculated from repeats of ilmenite reduction experiments carried out at 1000°C.

Reaction temperature (°C)	Reduction reaction phase				Water release phase		
	Water production rate (μl hr^{-1})				Total corrected pressure change (mbar)	Total calculated water produced (μmol)	Total calculated water produced (μl)
	0-1 h	1-2 h	2-3 h	3-4 h			
850 ± 5	0.31±0.07	0.29±0.07	0.30±0.07	0.30±0.07	90 ± 7	60±5	1.08±0.08
900 ± 5	0.37±0.07	0.32±0.07	0.32±0.07	0.33±0.07	101 ± 7	68±5	1.22±0.08
950 ± 5	0.40±0.07	0.40±0.07	0.40±0.07	0.41±0.07	122 ± 7	82±5	1.47±0.08
1000 ± 5	0.46±0.07	0.47±0.07	0.47±0.07	0.48±0.07	143 ± 7	96±5	1.72±0.09
1050 ± 5	0.45±0.07	0.59±0.08	0.62±0.08	0.61±0.08	175 ± 7	117±5	2.11±0.09

1100 ± 5	0.53±0.08	0.65±0.08	0.62±0.08	0.63±0.08	186 ± 7	124±5	2.24±0.09

Table 2. *Water production rates for reduction of ~45 mg ilmenite in ~420 mbar hydrogen as a function of temperature between 850 to 1100°C. Values are calculated for each hour of reduction from the reaction phase data. The total water production rate over 4 hours is calculated from the water release phase data. The total corrected pressure change is also included.*

To confirm that water is being produced and condensed during the reaction, a mass spectrum of the produced volatiles was obtained. The volatiles were condensed at the cold finger and released into the system and through the capillary attached at valve 2 (Figure 1) upon heating. An example spectra of the m/z values of interest/those showing a distinct change is shown in Figure 4.

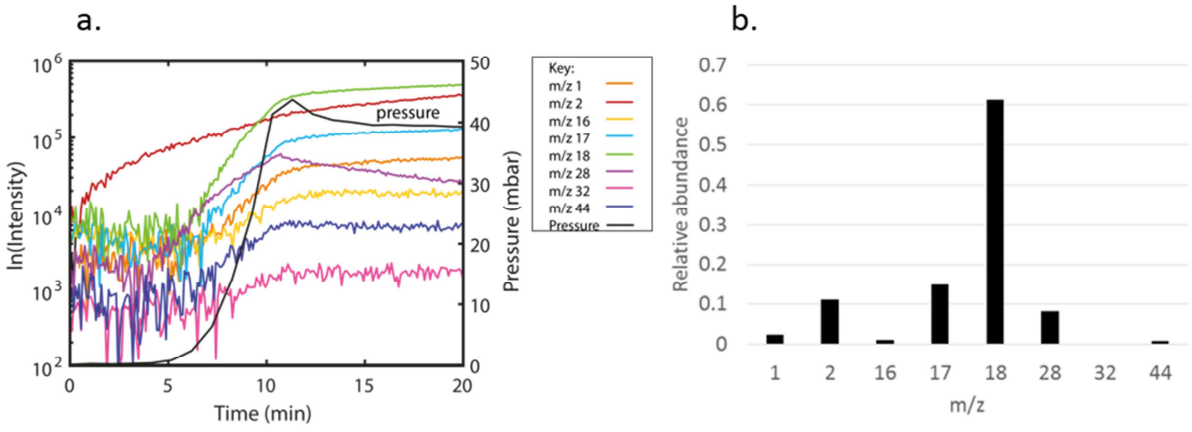

Figure 4. a.) *Mass spectrum with time during the heating of the cold finger to sublimate trapped water. The pressure increase during the release is also shown, along with data for m/z 1, 2, 16,*

17, 18, 32, and 44.. Background data has been removed. b.) Relative abundance of each m/z value as determined from the change in intensity and RSF factor.

It can be seen that there is a distinct increase in the intensity of certain m/z values as the pressure rises in the system (Figure 4a). Applying the relevant sensitivity factors, RSF (Hiden Analytical), to the change in intensity enables the determination fo relative abundance of each species (Figure 4b). The gas released upon heating the cold finger appears to be predominantly water, on account of its characteristic mass spectrum (m/z 16, 17,18) (NIST). There is also some residual hydrogen (m/z 1 & 2), and some carbon dioxide and carbon monoxide detected (m/z 44 & 32 respectively).

3.1.2 Yields

The yield in terms of oxygen wt. % and the reduction extent are calculated as in Section 2.3 and summarized in Figure 5. These outputs are calculated from the reaction phase data and are shown for each hour of the reaction. The final yield as calculated from the water release phase is also shown. Uncertainties are derived from the propagation of uncertainties of the quantity of water produced (Table 1), and the uncertainty in sample mass (±0.5 mg).

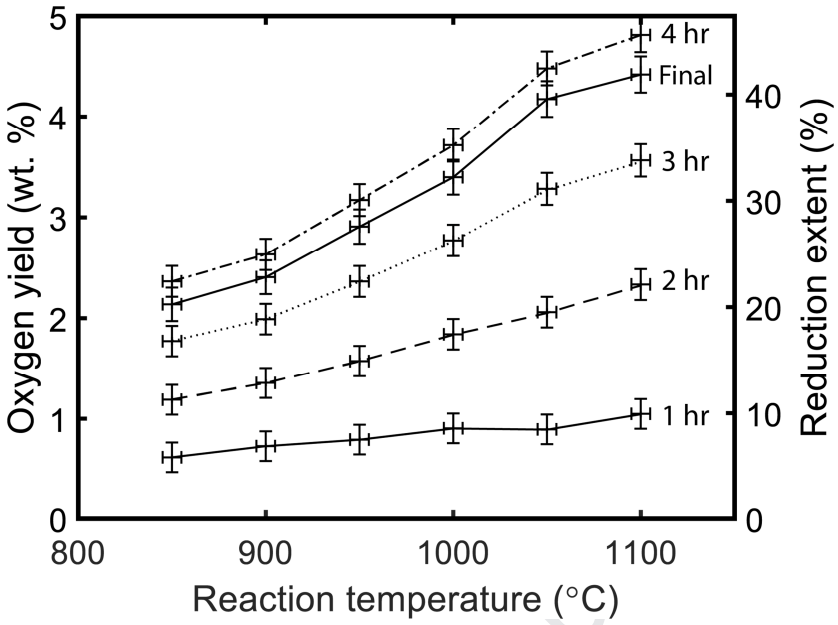

Figure 5. *The yield and reduction extent as calculated from the reaction phase for each hour of the reaction. The final yield/reduction extent is calculated from the water release phase data.*

The yields/reduction extent increases with temperature with the greatest yield at 1100°C. Final yields for the sample reacted at 1100°C as calculated from the release of water is 4.42±0.18 wt. % oxygen. Meanwhile the maximum extent of the reduction reactions after 4 hrs is 42.0±1.7%.

3.1.3 Sample Analysis

A ~15 mg sample of reacted ilmenite grains from each experiment is set in epoxy resin and polished for analysis. The samples are imaged at the Open University using the Scanning Electron Microscope (SEM) providing electron Back Scatter Electron (BSE) imaging. BSE images highlight differences in atomic mass of the elements in the sample and are used to identify the minerals present.

Example grains from the samples reacted at 1000°C, 1050°C, and 1100°C as imaged with BSD are shown in Figure 6. The grayscale contrast shows where the light gray ilmenite has reduced to form the darker gray rutile and the bright white iron. For the 1000°C sample it can be seen that voids have formed, a consequence of mass loss as oxygen is removed from the sample, as the reaction proceeds towards the middle of the grains. At 1050°C, the melting point of ilmenite, the reaction proceeds further into the grain and the rutile products appears to form vein-like features. Meanwhile, at 1100°C a titanium enriched solid solution forms within the grain (later identified as ferrospeudobrookite), often with a small unreacted core of ilmenite. Rutile is rare or absent, whilst the presence of metallic iron is clearly seen as bright features on the exterior grain surface as well as within the grain. The grains shown in Figure 6 were selected as they represent the majority of grains imaged in each sample.

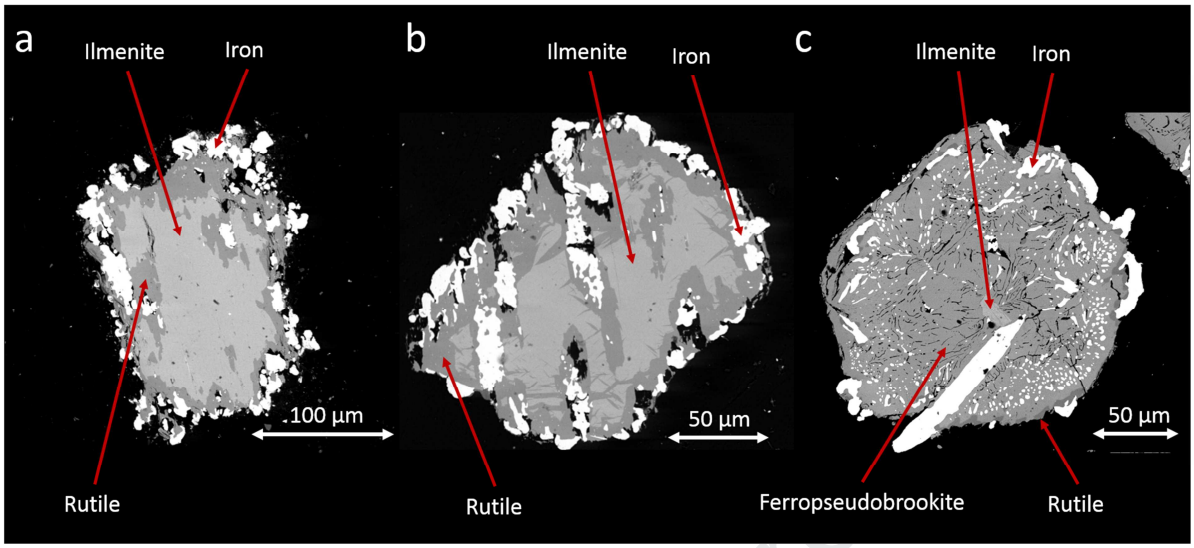

Figure 6. *BSE images of ilmenite grains reduced in the presence of hydrogen for 4 hours at a.) 1000°C, b.) 1050°C, c.) 1100°C. The reduction extent for each grain has been calculated as 32.3±1.6%, 39.7±1.7%, and 42.0±1.7% respectively.*

X-ray diffraction (XRD) was carried at out at the Natural History Museum, UK, and performed on ~5mg (~11%) of the 1000°C, 1050°C, and 1100°C reduction temperature samples to understand the phase of the mineral composition of the reacted grains (supplementary material Figure S4). The XRD analysis was performed using an Enraf-Nonius Powder Diffraction System 120 utilizing a CoKa1 radiation source. For the 1000°C sample all peaks can be explained by the presence of ilmenite, and the reduction products iron and rutile, indicating the sample is partially reduced. Meanwhile the 1100°C sample produced XRD peaks that indicate the presence of ferropseudobrookite ($FeTi_2O_5$), along with the iron, rutile, and ilmenite. The 1050°C sample is mostly comprised of ilmenite and its standard reduction products, rutile and iron, however there is also evidence to suggest that ferropseudobrookite is starting to form.

3.2 Hydrogen Concentration Studies

The following ilmenite reduction experiments were performed at 1000°C with varying hydrogen concentrations. The concentrations are defined as a ratio of n_h:n_{ilm}. Varying hydrogen concentrations from 0.28 up to 1.38 are trialled in this work, which equates to starting pressures of 118 mbar up to 584 mbar (when calculated for a manifold temperature of 120°C). With each experiment reacting 45 mg of ilmenite (0.3 mmol), the quantity of hydrogen required is calculated as a ratio of 0.3 mmol. The pressure was recorded during the reaction and release phase of each experiment. A blank reading was obtained for comparison by reacting an ilmenite sample at 1000°C with no hydrogen.

3.1.2 Reaction Pressures

The pressure changes during the 4 hour reaction phase show that initially, the lower the hydrogen concentration, the more water produced and condensed (Figure 7a). However, as the hydrogen supply is depleted, the reaction rate slows down. When the initial hydrogen concentration was lower, the reaction rate slows earlier. For example, in the first hour, the greatest pressure drop, and therefore the greatest production of water results from a 0.28:1.0 ratio of H_2:$FeTiO_3$ (n_h:n_{ilm}). However, as the reaction proceeds past 80 minutes, higher pressures of hydrogen are required to sustain faster reaction rates. As the n_h:n_{ilm} concentration exceeds 1, the reaction rate is not improved after 4 hours. The pressure data is shown in supplementary material Table S5, along with the calculated quantity of hydrogen reacted, n_h, using Eqn. 2.

The pressure change as a result of the water release phase shows that after 4 hours, the greatest production of water occurs as a result of a 0.99:1 concentration of n_h:n_{ilm}, which equates to a pressure of 418 mbar (Figure 7b). It does not highlight the variation in reaction rate across the 4

355 hr period as in Figure 7a. The pressure data for the water release phase is shown in
356 supplementary material Table S6.

357

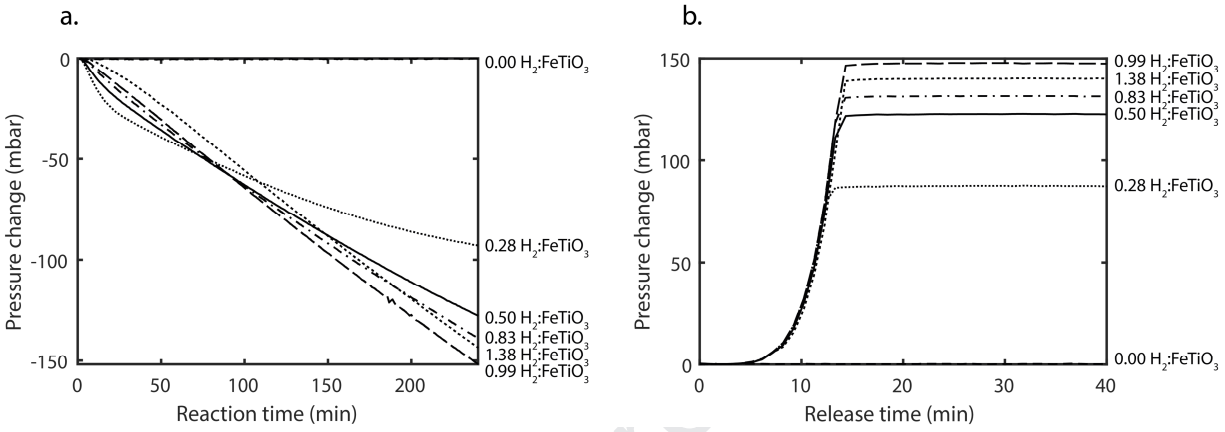

358

359 ***Figure 7.*** *Pressure change during a.) the ilmenite reduction reaction, and b.) the water release*
360 *phase, for varying initial H_2:$FeTiO_3$ concentrations. Results shown are not corrected for the*
361 *blank reading.*

362 The breakdown of water production rates during the reaction phase, and the total amount of
363 water produced as calculated form the water release phase are shown in Table 3. The water
364 production rate varies throughout the reaction, which is indicated in the estimates for the
365 changing reaction rate throughout the reaction. In the first hour, lower pressures of hydrogen are
366 desirable providing water produciton rates of up to 0.54±0.08 μl hr^{-1} when the ilmenite was
367 exposed to an initial pressure of 118 mbar of hydrogen. As the reaction proceeds into the fourth
368 hour, the studies in which higher intial hydrogen pressures were used result in the highest water
369 production rates of 0.49±0.07 μl hr^{-1} for the studies using both 418 mbar and 584 mbar of
370 hydrogen (0.99:1 and 1.39:1 n_h:n_{ilm} respectively). The water production rate as calculated from

371 the water release phase indicate that in a 4 hour reaction, the optimum initial pressure of
372 hydrogen is 418 mbar which equates to a 0.99:1 ratio of n_h:n_{ilm}.

373

Initial H_2 conditions		Reduction reaction phase				Water release phase		
		Water production rate (μl hr^{-1})				Total corrected pressure change (mbar)	Total calculated water produced (μmol)	Total calculated water produced (μl)
H_2:Ilmenite Concentration	H_2 Pressure (mbar)	0-1 h	1-2 h	2-3 h	3-4 h			
0.28:1.00	118±1	0.54±0.08	0.28±0.07	0.21±0.07	0.15±0.07	87±7	59±5	1.05±0.08
0.50:1.00	210±1	0.52±0.08	0.40±0.07	0.36±0.07	0.35±0.07	123±7	82±5	1.48±0.08
0.83:1.00	345±1	0.49±0.07	0.46±0.07	0.42±0.07	0.42±0.07	131±7	88±5	1.58±0.08
0.99:1.00	418±1	0.47±0.07	0.50±0.08	0.49±0.08	0.49±0.07	148±7	99±5	1.78±0.09
1.38:1.0	584±1	0.37±0.07	0.50±0.08	0.49±0.08	0.49±0.07	140±7	94±5	1.69±0.09

374 ***Table 3.*** *Water production rates for reduction of ~45 mg of ilmenite performed under variable*
375 *hydrogen concentration conditions at 1000°C. Values are calculated for each hour of reduction*
376 *from the reaction phase data. The total water production rate over 4 hours is calculated from the*
377 *water release phase data.*

378 **3.2.2 Yields**

379 The yield in terms of oxygen wt. % and the reduction extent are calculated as in Eqn. 4 and 5
380 respectively and the results are shown in Figure 8.

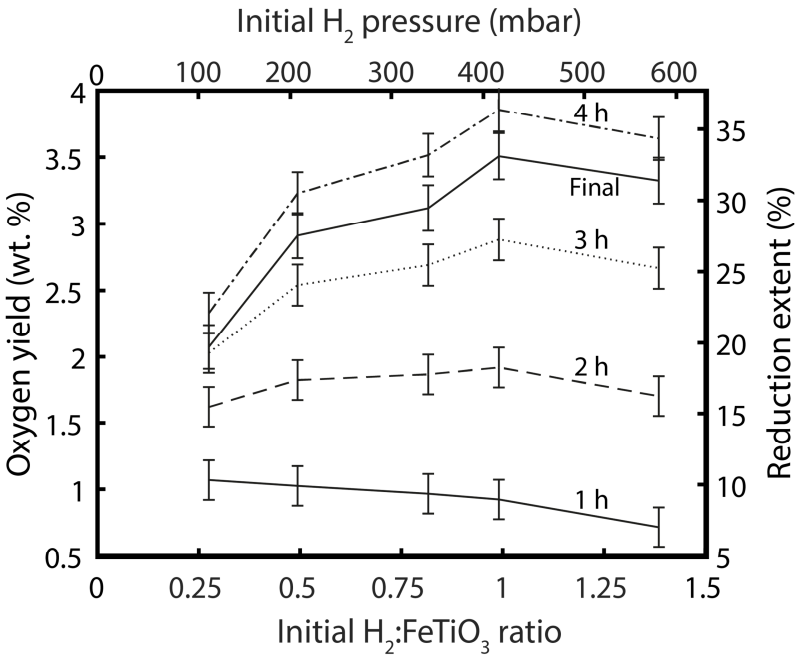

381

382 ***Figure 8.*** *The yield and reduction extent as calculated from the reaction phase for each hour of*
383 *the reaction. The final yield/reduction extent is calculated from the water release phase data.*

384

385 The yield/reduction extent is initially higher with lower quantities of hydrogen. However, the
386 maximum yield after 4 hours occurs when the initial n_h:n_{ilm} ratio is 0.99:1.0 which equates to a
387 hydrogen pressure of 418 mbar. The maximum final yield for this setup at a reaction temperature
388 of 1000°C and a hydrogen pressure of 418 mbar is 3.51±0.17 wt.% oxygen. Meanwhile the
389 maximum extent of the reduction reaction after 4 hours is 33.4±1.7 %.

4 Discussion

The setup of the ISRU-BDM is functionally identical to parts of ProSPA. Both systems are heated entirely along the lengths of the experimentally relevant sections and both systems will operate at similar temperatures, both for the IRSU reactions and subsequent processing of the resultant gas. However, the ISRU-BDM has been constructed using commercial components in order to test a specific reaction and is therefore not completely representative of the flight system. While most of the hardware is functionally identical, there are some differences that are significant. The ISRU-BDM is significantly larger than the ProSPA flight model and has more power available, allowing for the use of pneumatically actuated metal-tipped values as opposed to the electronically actuated polymer tipped valves that will ultimately be used. The use of these valves and the availability of appropriately sized components requires the use of pipes approximately twice the diameter of those that will be used in ProSPA. As a result, the conductance of the pipework, and therefore the gas diffusion rate, will be much lower in the ProSPA flight model than in the ISRU-BDM. This is likely to cause a decrease in reaction rate, although this will be partially offset by shorter diffusion pathways as a result of the overall smaller dimensions of ProSPA. The reaction rate is also likely to be affected by a difference in cooling mechanism between the two systems. The ISRU-BDM uses an active system based on liquid nitrogen to cool a cold finger, whereas ProSPA will rely on radiative losses to space in order to cool its cold fingers. The liquid nitrogen-based system requires cooling a large metal mass within the ISRU-BDM heated box, making the cooling process somewhat inefficient. At present, the performance of the radiative cooling system is not known so the differences in efficiency cannot be categorically stated. It is not envisioned that any of these variations from the ProSPA flight model will affect the viability of the ISRU experiments, although the reaction

rates are likely to differ. Other nominally significant hardware differences, such as the valves, are unlikely to materially affect the experiments.

The ISRU-BDM is more capable than the BDM used in Sargeant et al. (2019a) in efficiently trapping and releasing water for quantification. This is a consequence of the uniformly heated ISRU-BDM system of ~120°C which limits the condensation of the produced water onto the pipework. However, the pipework still appears to adsorb water and so higher temperatures and/or hydrophobic surface coatings would be required to improve the efficiency of the system in retrieving more of the water produced during the reaction. Providing the retrievable water results in measurable pressures, and a water calibration is performed on the final ProSPA system to determine how much water adsorption will occur, the adsorption effects will not limit the quantification of yields.

It is often stated that ilmenite reduction can be performed at temperatures of up to 1000°C, particularly in work relating to ISRU applications (e.g. Gibson & Knudsen, 1985; Li et al., 2012; Taylor & Carrier, 1993). The temperature studies performed using a static setup in this work, and those in the wider literature which utilize gas flowing systems (Li et al., 2012; Zhao & Shadman, 1993), show that with increasing temperature from 850 to 1100°C the reaction rate increases and yields higher quantities of water. Altenberg et al. (1993) also modelled how higher temperatures increase the equilibrium constant and ultimately the yield.

SEM and XRD analysis of the 1100°C sample shows the formation of ferropseudobrookite, $FeTi_2O_5$, indicating a different reaction has taken place as compared to Eqn. 1. Ferropseudobrookite is isostructural to Armalcolite, $(FeMg)Ti_2O_5$, and is known to form at low pressures and oxygen fugacities (Lindsley et al., 1974), which are also the conditions of the

experiments in this study. The following process has been considered to explain the production of ferropseudobrookite as part of the reduction reaction:

$$3FeTiO_{3(s)} + 2H_{2(g)} \rightleftharpoons 2Fe_{(s)} + TiO_{2(s)} + 2H_2O_{(g)} + FeTi_2O_{5(s)} \quad \textbf{Eqn. 6}$$

This process is a subsolidus reaction occurring at temperatures of at least 1050°C (Lindsley et al., 1974) and was demonstrated by Si et al. (2012) where the production of a M_3O_5-type solid solution was recorded, where M represents the elements Mg, Ti, and Fe. A higher ratio of n_h:n_{ilm} is required for the reaction to proceed to the right as written as compared to Eqn. 1, meaning more ilmenite is required to produce the equivalent amount of water. However, the trend in yield with reaction temperature does not appear to change significantly (Figure 5). There was no indication of a secondary reduction step where rutile reduces to a less oxidized state such as Ti_3O_5 (Bardi et al., 1987) supporting the literature which states that TiO_2 will only begin to reduce when all the ilmenite present has reduced (Zhao & Shadman, 1993).

Hydrogen pressures in the system appear to have a two-fold effect on the reaction. Initially, lower pressures produce the highest rates of water production at 0.54±0.08 μl hr^{-1} for a starting pressure of 118 mbar. Altenberg et al.'s (1993) model showed that lower hydrogen pressures equated to an increase in the equilibrium constant and therefore greater yields. However, after 1 hour, the highest rates of water production are measured at higher pressures where the starting pressure was 418 mbar. A model suggesting how hydrogen pressure affects reaction rate is shown in Figure 9. There are various pathways for gases to diffuse through minerals to enable the reduction reaction to continue to the right as written. Such pathways include the movement of vacancies within the mineral structure or via movement through the interstitial structure (Watson & Baxter, 2007). However, when reduction of the outer ilmenite grain occurs, the mineral structure loses mass and voids form which facilitate further movement of gases into and out of

459 the grain (Figure 5a) as seen in Dang et al. (2015) and Li et al. (2012). The slowing of the
460 reaction rate as the reaction proceeds to the interior of the grain suggests that the diffusion of
461 gases through the grain is the rate controlling step. A batch mode process which implements low
462 pressures at the start of the reaction and higher pressures as the reaction proceeds would be worth
463 further investigation.

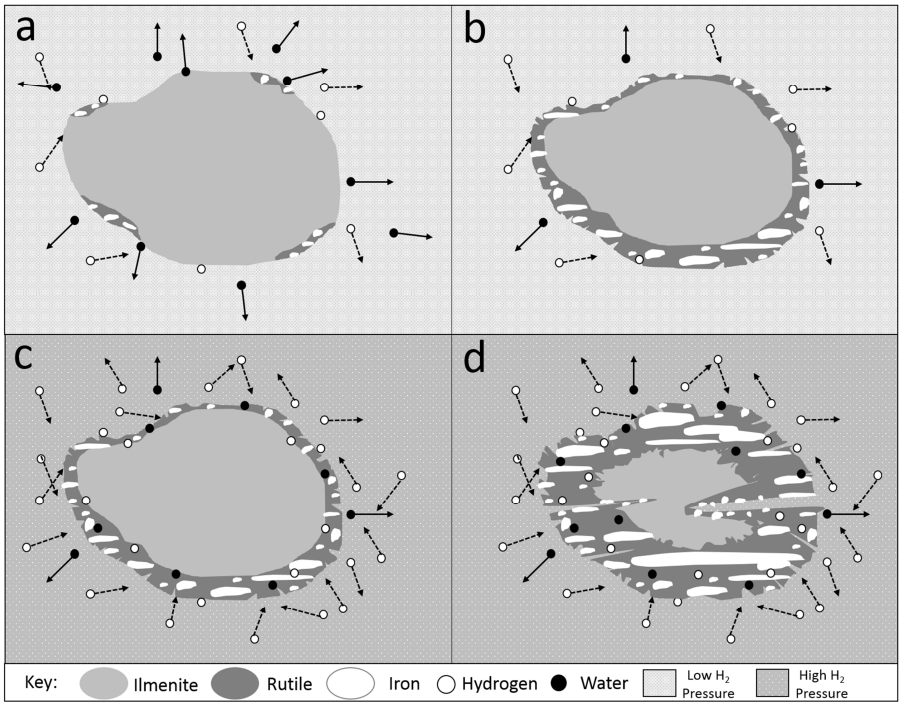

464

465 ***Figure 9.*** *The effects of hydrogen pressure on the reaction rate during the reduction of ilmenite.*
466 *a.) low hydrogen pressures initially is sufficient to reduce the readily available surficial ilmenite,*
467 *whilst the produced water can easily diffuse away from the reaction site to the cold finger. b.) as*
468 *the reaction proceeds, the low hydrogen pressure is not sufficient to penetrate through the*
469 *reaction products to react with the internal ilmenite. c.) when the outer grain has reacted, higher*
470 *pressures are needed to penetrate through the reaction products. d.) the reaction is then able to*

proceed further into the grain, however, it will take longer for the produced water to diffuse away from the reaction site compared to the start of the reaction.

The ilmenite used in this work is of terrestrial origin. Terrestrial ilmenite contains ~6% Fe^{3+}, whereas lunar ilmenite contains none and would therefore require more hydrogen in order to produce equivalent quantities of water to lunar ilmenite. However, terrestrial ilmenite has ~2% magnesium, compared to ~6% for lunar ilmenite in the mineral structure and would therefore react to produce more water per unit weight compared to lunar ilmenite (Deer et al., 1992). Considering the small quantities of ilmenite expected in the bulk lunar material and the counteracting factors effecting the yield of water from terrestrial ilmenite to lunar ilmenite, it is assumed that terrestrial ilmenite is a suitable proxy for lunar ilmenite in this study.

This study was performed to understand if and how a static system of the ProSPA design could be used to reduce lunar minerals with hydrogen. Ilmenite was selected for use with the study as it is a common lunar mineral that can be readily reduced, however, this process is not expected to produce equivalent yields with lunar regolith. If the experimental procedure outlined in this study were to be applied on the Moon, the yields would be significantly reduced. Although lunar regolith is thought to contain as much as 20% by volume ilmenite (Warner et al. 1978, Chambers et al. 1995, Papike et al. 1998, Hallis et al. 2014), it is thought that in the lunar highland regions, ilmenite concentrations can be <1% by volume (Taylor et al., 2010). Other lunar minerals that contain FeO can also be reduced, such as pyroxene, olivine, and iron-rich volcanic glass (Allen et al., 1994). Therefore, even if ProSPA samples highland material it should be possible to reduce lunar minerals to produce water on the Moon for the first time.

5 Conclusions

A breadboard model of the ProSPA instrument has been constructed and used to optimize the ISRU experiments planned to be performed on the lunar surface. Such experiments would include the reduction of lunar simulants, meteorites and Apollo samples, in preparation for application on the Moon. In this study ilmenite, a common lunar mineral, is used to optimize the reaction procedure. Increasing reaction temperature results in greater yields, where reaction temperatures of ≥1500°C result in an alternative reaction process with the formation of ferropseudobrookite. The results have shown that the reduction reaction does not complete within 4 hours at temperatures between 850 and 1100°C. The samples reduced at 1000°C show a reduction extent of 32.3±1.6 % in 4 hours with a maximum yield of 3.40±0.17 wt. % O_2 from ~45 mg ilmenite, producing a total of 1.72±0.09 µl of water. The highest yields were recorded at 1100°C where the ilmenite grains undergo a subsolidus reaction forming ferropseudobrookite resulting in a reduction extent of 42.0±1.7% in 4 hours with a maximum yield of 4.42±0.18 wt. % O_2, producing a total of 2.24±0.09 µl of water.

Hydrogen concentration has varying effects on the reduction reaction when reducing ~45 mg of ilmenite at 1000°C. Lower hydrogen pressures (118 mbar equating to a ratio of 0.28:1.00 n_h:n_{ilm}) showed greater reaction rates in the first hour of the reaction producing water at a rate of 0.54±0.08 µl hr^{-1}. However, as the reaction proceeds, higher pressures are required, equating to a starting pressure of 418 mbar (equivalent to a ratio of 0.99:1.00 n_h:n_{ilm}) resulting in a water production rate of 0.49±0.07 µl hr^{-1} in the fourth hour of the reaction. A 'batch mode' reaction will be considered in future work where higher pressures of hydrogen are added to the system throughout the reaction to increase the reaction rate.

Acknowledgements

The authors would like to acknowledge the support of Jens Najorka for support in performing XRD analyses at the Natural History Museum, London, UK. The authors also acknowledge the support of Dr Giulia Degli-Alessandrini for assistance with operating the SEM, and Dr Aiden Cowley for supplying the ilmenite used in the experiments. Two anonymous reviewers are thanked for their critical analysis of the manuscript. This work was supported by a Science and Technology Facilities Council (STFC) studentship grant [grant number ST/N50421X/1] to Hannah Sargeant and by The Open University. Mahesh Anand and Simeon Barber acknowledge support from UKSA grant #ST/R001391/1. ProSPA is being developed by a consortium led by The Open University, UK, under contract to the PROSPECT prime contractor Leonardo S.p.A., Italy, within a programme of and funded by the European Space Agency.

References

Allen, C. C., Morris, R. V., & McKay, D. S. (1994). Experimental reduction of lunar mare soil and volcanic glass. Journal of Geophysical Research: Planets, 99(E11), 23173-23185. https://doi.org/10.1029/94JE02321

Altenberg, B., Franklin, H., & Jones, C. (1993). *Thermodynamics of lunar ilmenite reduction.* Paper presented at the Proceedings of the Lunar and Planetary Science Conference XXIV, Houston, TX.

Barber, S. J., Wright, I. P., Abernethy, F., Anand, M., Dewar, K. R., Hodges, M., . . . Trautner, R. (2018). *ProSPA: Analysis of Lunar Polar Volatiles and ISRU Demonstration on the Moon.* Paper presented at the Proceedings of the 49th Lunar and Planetary Science Conference, Houston, TX

Bardi, G., Gozzi, D., & Stranges, S. (1987). High temperature reduction kinetics of ilmenite by hydrogen. *Materials chemistry and physics*, 17(4), 325-341. https://doi.org/10.1016/0254-0584(87)90085-X

Barnes, J. J., Tartèse, R., Anand, M., McCubbin, F. M., Franchi, I. A., Starkey, N. A., & Russell, S. S. (2014). The origin of water in the primitive Moon as revealed by the lunar highlands samples. *Earth and Planetary Science Letters*, 390, 244-252. https://doi.org/10.1016/j.epsl.2014.01.015

Burke, J. D. (2012). 'Perpetual Sunshine, Moderate Temperatures and Perpetual Cold as Lunar Polar Resources', in Badescu, V. (Ed.) *Moon.* New York: Springer, pp. 335-345. https://doi.org/10.1007/978-3-642-27969-0

548 Chambers J. G., Taylor L. A., Patchen A., McKay D. S. (1995) Quantitative mineralogical
549 characterization of lunar high-Ti mare basalts and soils for oxygen production. *Journal of*
550 *Geophysical Research*, 100, 14391-14401. https://doi.org/10.1029/95JE00503
551 Christiansen, E., Simonds, C. H., & Fairchild, K. (1988). Conceptual design of a lunar oxygen
552 pilot plant. LPI Contributions, 652, 52.
553 Colaprete, A., Schultz, P., Heldmann, J., Wooden, D., Shirley, M., Ennico, K., . . . Elphic, R. C.
554 (2010). Detection of water in the LCROSS ejecta plume. *Science*, 330(6003), 463-468.
555 https://doi.org/10.1126/science.1186986
556 Dang, J., Zhang, G.-h., & Chou, K.-c. (2015). Kinetics and mechanism of hydrogen reduction of
557 ilmenite powders. *Journal of Alloys and Compounds*, 619, 443-451.
558 https://doi.org/10.1016/j.jallcom.2014.09.057
559 Deer, W. A., Howie, R. A., & Zussman, J. (1992). An introduction to the rock-forming minerals
560 (2nd ed.). Essex, England: Pearson Education Limited.
561 Gibson, M. A., & Knudsen, C. W. (1985). *Lunar oxygen production from ilmenite*. Paper
562 presented at the Lunar bases and space activities of the 21st century, Houston, TX.
563 Hallis L. J., Anand M., Strekopytov S. (2014) Trace-element modelling of mare basalt parental
564 melts: Implications for a heterogeneous lunar mantle. Geochimica et Cosmochimica
565 Acta, (134) 289-316. https://doi.org/10.1016/j.gca.2014.01.012
566 Hiden Analytical. Relative Sensitivity, RS Measurements of Gases. Gas Analysis, Application
567 Note 282. Retrieved from: https://www.hiden.de/wp-
568 content/uploads/pdf/RS_Measurement_of_Gases_-
569 _Hiden_Analytical_App_Note_282.pdf. Accessed on 25/07/2019.

570 Jones, H. W., & Kliss, M. H. (2010). Exploration life support technology challenges for the
571 Crew Exploration Vehicle and future human missions. *Advances in Space Research*,
572 45(7), 917-928. https://doi.org/10.1016/j.asr.2009.10.018
573 Latham, G. V., Ewing, M., Press, F., Sutton, G., Dorman, J., Nakamura, Y., . . . Duennebier, F.
574 (1970). Passive seismic experiment. *Science*, 167(3918), 455-457.
575 https://doi.org/10.1126/science.167.3918.455
576 Lewis J. S., M. D. S. a. C. B. C. (1993). 'Using Resources from Near-Earth Space', In J. S.
577 Lewis, M. S. Matthews, & M. L. Guerrieri (Eds.) *Resources of Near-Earth Space*
578 London: University of Arizona Press, pp. 3-14.
579 Li, S., Lucey, P. G., Milliken, R. E., Hayne, P. O., Fisher, E., Williams, J.-P., . . . Elphic, R. C.
580 (2018). *Direct evidence of surface exposed water ice in the lunar polar regions.*
581 Proceedings of the National Academy of Sciences(115), 8907-8912.
582 https://doi.org/10.1073/pnas.1802345115
583 Li, Y., Li, X., Wang, S., Tang, H., Gan, H., Li, S., . . . Ouyang, Z. (2012). 'In-situ water
584 production by reducing ilmenite' in Badescu, V. (Ed.) *Moon.* New York: Springer, pp.
585 189-200. https://doi.org/10.1007/978-3-642-27969-0
586 Lindsley, D., Kesson, S., Hartzman, M., & Cushman, M. (1974). *The stability of armalcolite-*
587 *Experimental studies in the system MgO-Fe-Ti-O*. Paper presented at the Lunar and
588 Planetary Science Conference Proceedings, Houston, TX
589 Maxwell, J., Peck, L., & Wiik, H. (1970). *Chemical composition of Apollo 11 lunar samples*
590 *10017, 10020, 10072 and 10084.* Paper presented at the Apollo 11 Lunar Science
591 Conference, Houston, TX.

McCubbin, F. M., Vander Kaaden, K. E., Tartèse, R., Klima, R. L., Liu, Y., Mortimer, J., . . . Lawrence, D. J. (2015). Magmatic volatiles (H, C, N, F, S, Cl) in the lunar mantle, crust, and regolith: Abundances, distributions, processes, and reservoirs. *American Mineralogist*, 100(8-9), 1668-1707. https://doi.org/10.2138/am-2015-4934CCBYNCND

Ness Jr, R. O., Sharp, L. L., Brekke, D. W., Knudsen, C. W., & Gibson, M. A. (1992). *Hydrogen reduction of lunar soil and simulants.* Paper presented at the Engineering, Construction, and Operations in space-III: Space'92.

NIST. Water, Mass spectrum (electron ionization). Retrieved from: https://webbook.nist.gov/cgi/cbook.cgi?ID=C7732185&Mask=200#Mass-Spec. Accessed on 25/07/2019.

Papike, Taylor, L., & S, S. (1991). Lunar Minerals. In G. Heiken, D. Vaniman, & B. M. French (Eds.), Lunar sourcebook (pp. 121-181). ISBN 0-521-33444-6

Saal, A. E., Hauri, E. H., Cascio, M. L., Van Orman, J. A., Rutherford, M. C., & Cooper, R. F. (2008). Volatile content of lunar volcanic glasses and the presence of water in the Moon's interior. *Nature*, 454(7201), 192. https://doi.org/10.1038/nature07047

Sanders, G. B., & Larson, W. E. (2011). Integration of in-situ resource utilization into lunar/Mars exploration through field analogs. *Advances in Space Research*, 47(1), 20-29. https://doi.org/10.1016/j.asr.2010.08.020

Sargeant, H. M., Abernethy, F., Anand, M., Barber, S. J., Landsberg, P., Sheridan, S., . . . Morse, A. (2019a). Hydrogen Reduction of Ilmenite in a Static System for use as an ISRU Demonstration on the Lunar Surface. *Planetary and Space Science* (In Review).

Sargeant, H. M., Abernethy, F., Anand, M., Barber, S. J., Sheridan, S., Wright, I. P., & Morse, A. (2019b). *Experimental development and testing of the ilmenite reduction reaction for a*

615 *lunar ISRU demonstration with ProSPA.* Paper presented at the Lunar and Planetary
616 Science Conference L, Houston, TX.
617 Sefa, M., Setina, J., & Erjavec, B. (2014). A new method for determining water adsorption
618 phenomena on metal surfaces in a vacuum. *Materials and technology*, 48(1), 119-124.
619 Si, X.-g., Lu, X.-g., Li, C.-w., Li, C.-h., & Ding, W.-z. (2012). Phase transformation and
620 reduction kinetics during the hydrogen reduction of ilmenite concentrate. *International*
621 *Journal of Minerals, Metallurgy, and Materials*, 19(5), 384-390.
622 https://doi.org/10.1007/s12613-012-0568-4
623 Taylor, L. A., Pieters, C., Patchen, A., Taylor, D. H. S., Morris, R. V., Keller, L. P., & McKay,
624 D. S. (2010). Mineralogical and chemical characterization of lunar highland soils:
625 Insights into the space weathering of soils on airless bodies. Journal of Geophysical
626 Research: Planets, 115(E2). https://doi.org/10.1029/2009JE003427
627 Taylor, L., & Carrier, W. (1993). 'Oxygen Production on the Moon: An Overview and
628 Evaluation' , In J. S. Lewis, M. S. Matthews, & M. L. Guerrieri (Eds.) *Resources of*
629 *Near-Earth Space* London: University of Arizona Press, pp. 69-108
630 Warner R. D., Nehru C. E., Keil K. (1978) Opaque oxide mineral crystallization in lunar high-
631 titanium mare basalts. American Mineralogist 63, 1209-1224.
632 Watson, E. B., & Baxter, E. F. (2007). Diffusion in solid-Earth systems. Earth and Planetary
633 *Science Letters*, 253(3-4), 307-327. https://doi.org/10.1016/j.epsl.2006.11.015
634 Weston, G. F. (1985). 'Chapter 1 - Fundamentals of vacuum science and technology' In G.F.
635 Weston (Ed.), *Ultrahigh vacuum practice*. London, UK: Butterworth & Co. Ltd., pp. 1-21
636 https://doi.org/10.1016/B978-0-408-01485-4.50004-0

637 Williams, R. J. (1985). *Oxygen extraction from lunar materials: An experimental test of an*
638 *ilmenite reduction process.* Paper presented at the Lunar bases and space activities of the
639 21st century.
640 Zhao, Y., & Shadman, F. (1993). 'Production of Oxygen from Lunar Ilmenite' , In J. S. Lewis,
641 M. S. Matthews, & M. L. Guerrieri (Eds.) *Resources of Near-Earth Space* London:
642 University of Arizona Press, pp. 149-178

Highlights:

- Demonstration of reduction of ilmenite by H_2 in a non-flowing system
- Proof of principle for an ISRU demonstration on the Moon
- Yields of up to 4.4 wt.% O_2 which is reasonable considering the constraints

Conflict of interest statement:

This work was supported by a Science and Technology Facilities Council (STFC) studentship grant [grant number ST/N50421X/1] to Hannah Sargeant and by The Open University. Mahesh Anand and Simeon Barber acknowledge support from UKSA grant #ST/R001391/1. ProSPA is being developed by a consortium led by The Open University, UK, under contract to the PROSPECT prime contractor Leonardo S.p.A., Italy, within a programme of and funded by the European Space Agency.